Research Article

Journal of Environmental Nanotechnology

Cytotoxicity Screening and Antibacterial Activity of Bio-inspired $Fe_{1-2x}Mg_xCo_x$ Nanoparticles by *Psidium guajava* Plant Extract

T. Vandhana*, G. Rajeshwaran, J. Hariharasudhan, Nipuna Ashok, S. Aravind Kumar and Nivin Shree

Department of Physics, PSG College of Arts and Science, Coimbatore, TN, India

Received: 04.08.2025 Accepted: 27.09.2025 Published: 30.09.2025

*vandhana@psgcas.ac.in

ABSTRACT

An eco-friendly method was adopted using *Psidium guajava* plant leaves extract to synthesize $Fe_{1-2x}Mg_xCo_x$ nanoparticles. High crystallinity, spherical shape, functional groups, Fe content, and the stability of nanoparticles were confirmed through characterization techniques such as XRD, FESEM-EDS, UV-visible, FTIR, FT-Raman, and Zeta potential. Furthermore, the $Fe_{1-2x}Mg_xCo_x$ nanoparticles were tested for biomedical applications. Antibacterial assays demonstrated enhanced activity against *Listeria monocytogenes* (Gram-positive) compared to *Serratia marcescens* (Gram-negative), attributed to differences in cell wall structure. Cytotoxicity analysis revealed that the synthesized $Fe_{1-2x}Mg_xCo_x$ nanoparticles induced a higher inhibitory effect on HeLa cells than on MCF-7 cells, confirming their potential anticancer efficacy. The synergistic combination of Fe, Mg, and Co ions significantly improved biological functionality, while *P. guajava* phytochemicals provided eco-friendly synthesis and surface stabilization. These findings highlight the potential of *P. guajava*-mediated $Fe_{1-2x}Mg_xCo_x$ nanoparticles as multifunctional agents for antibacterial and anticancer applications. The nanoparticles showed a greater efficacy for MCF-7 cells than HeLa cells. Also, $Fe_{1-2x}Mg_xCo_x$ nanoparticles didn't affect the normal cells, suggesting that can act as a potent bio-interface in the medical field.

Keywords: *Psidium guajava*; $Fe_{1-2x}Mg_xCo_x$ nanoparticles; Cytotoxicity; Antibacterial activity.

1. INTRODUCTION

Nanotechnology refers to the design and application of materials, systems, and devices at the nanometer scale, extending developments achieved at the macro- and micro-levels (Salata, 2004). Over the past decade, nanomaterials have progressed from being largely of academic interest due to their unique properties to achieving broad adoption in scientific research and commercial applications (Feynman, 2003). The structure and synthesis route of nanomaterials govern their specific responses in different applications (Ramos *et al.* 2017; Saji *et al.* 2010). Nanoparticles vary in size over a significant range, showing their scientific potential, which helps to bridge the gap between bulk and atomic materials. Particles at the nano-size level offer various applications in disciplines such as biology, chemistry, physics, material science, industries, etc., especially in the biomedical field. Nanoparticles find use in drug-delivery, encapsulation of drugs and enhance bioactivity. In pharmaceuticals, nanoencapsulation increases the efficiency and stability of the drugs (Hamidi *et al.* 2008; Labhasetwar and Pelecky, 2007). As the nanoparticles range from 1 - 100nm, with unique properties, the nanodrugs can be easily encapsulated, dissolved, entrapped, and delivered to various parts of the body, such as the brain, liver, kidney, etc (Chambers and Mitragotri, 2007; Khalkhali *et al.* 2019). On the basis of the preparation method, various forms of nanospheres and nanocapsules can be obtained (Zahin *et al.* 2019; Pu *et al.* 2019; Tan *et al.* 2019).

Synthesis of nanoparticles can be achieved from different methods, such as chemical, physical, thermal, and biological methods. Among all the methods, the biological method is preferred due to its advantageous properties (Banerjee *et al.* 2014; Maliekkal *et al.* 2018). For synthesizing stable, size-controlled, non-toxic nanomaterials, biological methods will be the best. Nanoparticles can be synthesized by biological methods, using various bio-entities, such as, plant byproducts and biomolecules (Navaladian *et al.* 2007). Nanoparticles synthesised using eco-friendly methods, termed “Green synthesis,” accompany green chemistry principles. Green synthesis of nanoparticles using plant extracts has emerged as a simple, non-toxic and eco-friendly method

(Sharma and Gupta, 2023). This biogenic route avoids toxic chemicals and provides a sustainable alternative for nanoparticle fabrication. Using the green synthesis method, highly stable nanoparticles can be obtained with a one-step process. Synthesis using plants provides a better option as they are non-toxic and contain a natural capping agent (Ramteke *et al.* 2013; Singh *et al.* 2018). Plants contain various phytochemicals such as flavonoids, carotenoids, saponins, tannins, carbohydrates, auxin, and gibberellins, which are responsible for reducing the metal ions to form nanoparticles and stabilizing them (Phanjom and Ahmed, 2015; Vinod *et al.* 2011). Nanoparticles produced through green methods with a non-toxic nature, inexpensive will be more favourable for biomedical applications. Various types of nanoparticles have been synthesized using plant-mediated methods for applications in the biomedical field (Raj *et al.* 2018; Saeed *et al.* 2018).

Various plants such as *Coriandrum sativum* (Narayanan and Sakthivel, 2008), *Aloe barbadensis* (Phokha and Seraphin, 2015; Yamamoto *et al.* 2007), *Citrus limon* (Prathna *et al.* 2011), *Medicago sativa* (Torresdey *et al.* 2002), *Avena sativa* (Armendariz *et al.* 2004), *Ocimum sanctum* (Philip and Unni, 2011), *Azadirachta indica*, *Cymbopogon flexuosus* (Shankar *et al.* 2005) and *Brassica juncea* (Haverkamp and Marshall, 2009) have been used to synthesize nickel, cobalt, copper, zinc and silver nanoparticles (Devi and Singh, 2014; Anastas and Warner, 1998). Many metal nanoparticles are being developed for biomedical applications as the metallic nanoparticles have the ability to target only affected tissue, leaving no harm to the normal tissue, which makes them unique and effective as a drug. Besides all these metal nanoparticles, magnetic nanoparticles made their place in various biomedical applications as *in vivo* imaging (Gao *et al.* 2004), hyperthermia (Sengupta *et al.* 2005), cancer therapy (Popovic and Brundin, 2006), respiratory disease, etc. Hence, due to their high magnetic behaviour, iron nanoparticles can behave as a potent medicine (Huh *et al.* 2005; Anderson *et al.* 2019). Fe-based nanoparticles have gained significant attention because of their magnetic nature and wide range of biomedical applications (Rajendran *et al.* 2024). The development of bimetallic and multimetallic nanoparticles has gained increasing attention due to their superior and tunable physicochemical properties compared to monometallic systems, enabling broader functional and application-specific performance. Examples include Fe–Pt (Chou *et al.* 2010), Co–Pt (Shevchenko *et al.* 2003), Fe–Co, and Co–Ni-based nanoparticles (Yin *et al.* 2013) synthesized via thermal decomposition methods, as well as Cd–Mg–Co-doped ZnO nanostructures investigated for their optical properties (Kalu *et al.* 2020).

Among various plant sources, *Psidium guajava* (guava) leaves are rich in secondary metabolites such as flavonoids, tannins and polyphenols which act as reducing and stabilizing agents during synthesis (Rani and Singh, 2021). These phytochemicals enhance particle stability and biocompatibility, making *P. guajava*-mediated synthesis a promising approach for biomedical nanomaterials. *Psidium guajava*, known commonly as guava, belongs to the Myrtaceae family, found in different parts of tropical areas. Its parts, such as roots, leaves, and fruit are used for different purposes (Venugopal, 2017). Guava is known for its antibacterial activity and medicinal uses in curing intestinal diseases. Guava showed significant antibacterial activity against common food-borne diarrhoea-causing bacteria and food spoilage bacteria (Gutiérrez *et al.* 2008). GC-MS analysis showed that *Psidium guajava* is enriched with phytochemicals such as flavonoids, tannins, carbohydrates, and essential oils, which are used as a reducing agent in the formation of nanoparticles (Arima and Danno, 2002; Xu *et al.* 2018).

In this work, *Psidium guajava* was used to synthesize $Fe_{1-2x}Mg_xCo_x$ nanoparticles using a green synthesis method. The novelty of this study lies in introducing a ternary combination of Fe–Mg–Co doped nanoparticle system stabilized by guava extract, designed to address the gap of dual antibacterial and anticancer activity in plant-mediated nanoparticles. The prepared nanoparticles were studied for antibacterial and *in vitro* cytotoxicity studies against bacterial pathogens and malignant cancer cells.

2. EXPERIMENT

2.1 Preparation of Plant Extract

Fresh leaves of the *Psidium guajava* plant were collected from the home premises, Tiruchirapalli, Tamil Nadu. These leaves (20 g) were washed thoroughly with distilled water, then finely chopped and dried in a dark room for two days to remove the debris. Then, the dried leaves were boiled for 20-25 minutes in 50 mL distilled water in a magnetic stirrer. When a colour change was observed, the solution was filtered and stored at 5°C for further use.

2.2 Preparation of $Fe_{1-2x}Mg_xCo_x$ Nanoparticles

For the synthesis of $Fe_{1-2x}Mg_xCo_x$ nanoparticles, biogenic method was adopted involving a simple single-step co-precipitation method with the plant extract. These nanoparticles were prepared with three different concentrations: sample S1 (x=0.1), S2 (x=0.15), and S3 (x=0.2). The nitrate precursors of Fe, Mg, and Co were mixed in distilled water at three different concentrations

and stirred on a magnetic stirrer for approximately 2 h. Subsequently, 10 mL of freshly prepared *Psidium guajava* extract was added dropwise to the solution until the pH reached ~9, which was adjusted and maintained using 0.1 M NaOH and monitored with a calibrated digital pH meter. The observed colour change in the solution indicated the formation of $Fe_{1-2x}Mg_xCo_x$ nanoparticles, primarily resulting from the reduction of metal ions by phytochemicals present in the plant extract, which act as both reducing and stabilizing agents. The formed nanoparticles were dried overnight in a hot air oven and then powdered in a mortar and kept in a sample collector for further studies.

2.3 Characterization Techniques

The bio-synthesized $Fe_{1-2x}Mg_xCo_x$ nanoparticles were characterised by different characterisation techniques. The crystallinity and crystal structure were analysed by XRD (PANalytical, X'Pert-PRO MPD) performed using Cu Kα radiation (λ = 1.54 Å). The surface morphology, particle size, and chemical composition of the samples were determined by Energy Dispersive X-ray analysis (EDS) with a Zeiss Sigma FESEM apparatus. The spectral analysis was carried out using a Vertex 70v FTIR spectrophotometer (BRUKER USA) in the range 4000 cm^{-1} - 500 cm^{-1}, and a Raman spectrum was obtained by using a Lab RAM HR (UV) system with excitation of 1063 nm near IR laser light. The optical properties of the samples were identified using a Jasco V530 UV-visible spectrophotometer. The stability of the samples was determined using the Zetasizer nano series (Malvern) instrument in the range 0.1 - 1000 µm.

2.4 Antimicrobial Assay

Agar-well diffusion method was employed to determine the antibacterial activity of as-synthesized $Fe_{1-2x}Mg_xCo_x$ nanoparticles. The antibacterial activity of the prepared samples was tested on *Listeria monocytogenes* (Gram positive) and *Serratia marcescens* (Gram negative) bacterial strains. About 20 mL of nutrient agar medium was poured into the Petri dish and inoculated for 24 hours with the strains. Then, the synthesized $Fe_{1-2x}Mg_xCo_x$ nanoparticles (S1, S2, and S3) of various concentrations (60 µg/mL, 40 µg/mL, and 20 µg/mL) were added to the plate and incubated at 37°C for another day. The diameter of the inhibition zone formed around the strains was measured, and antibacterial activity was assayed.

2.5 *In vitro* Cytotoxicity Assay

The bio-reduced $Fe_{1-2x}Mg_xCo_x$ nanoparticles were further subjected to *in vitro* cytotoxicity through MTT assay with ten different concentrations for each samples S1, S2, and S3 against the cultured MCF-7 cell lines (breast cancer) and HeLa cells lines (Human cervical carcinoma). The cells were maintained in Dulbecco's Modified Eagle Medium (DMEM) supplemented with 100 µg/mL penicillin, 10% Fetal Bovine Serum (FBS), and 100 µg/mL streptomycin, and kept under an atmosphere of 5% CO_2 at 37°C. Cultured cells were accumulated by trypsinization and blended in a 15 mL tube. The cells were plated at a density of 1×10^5 cells/ml (200 µL) into the 96-well tissue culture plate. Then, 20 µL of 5 mg/ml MTT was added to each well, and for another 2-4 hours, incubation continued. Finally, the absorbance was measured for each well using a microplate reader at 570 nm. Furthermore, the IC_{50} values were calculated for each sample using GraphPad Prism software. The cell viability and cytotoxicity were measured after the incubation for 48 hours for all the samples using the formula

$$\text{Cell viability\%} = \text{Mean OD Controlled OD} * 100 \quad \ldots (1)$$

$$\text{Cytotoxicity (\%)} = 100 - \text{Cell viability (\%)} \quad \ldots (2)$$

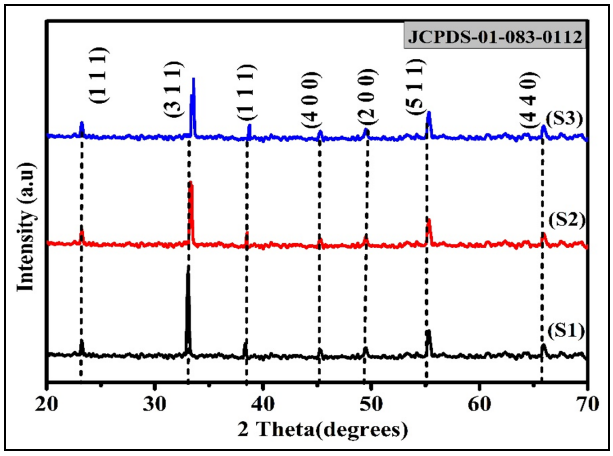


Fig. 1: XRD diffraction pattern of $Fe_{1-2x}Mg_xCo_x$ nanoparticles for S_1, S_2, S_3

3. RESULTS AND DISCUSSION

3.1 X-ray Diffraction

Fig. 3.1 shows the XRD pattern of the synthesised $Fe_{1-2x}Mg_xCo_x$ nanoparticles for all three samples, S1, S2, and S3. Well-defined peaks were observed at 2θ = 23.25°, 33.03°, 49.45°, 52.28°, 65.9°, attributed to planes (1 1 1), (3 1 1), (2 0 0), (5 1 1) and (4 4 0), corresponding to the FCC structure of a maghemite with ICSD card no. (01-083-0112) (Iconaru *et al.* 2013). Also, two additional peaks were observed at 2θ = 39.3°,45.25°, corresponding to (1 1 1) and (4 0 0) respectively, and no impurity peaks were observed, indicating high purity of the synthesised nanoparticles

(Sutapa *et al.* 2018). Mild shift with decrease in intensity was observed from S1 to S3 with the increase in concentration, and average crystalline size was calculated by Debye-Scherrer's formula, which was found to be 54.16 nm (S1), 54.21 nm (S2), and 54.4 nm (S3).

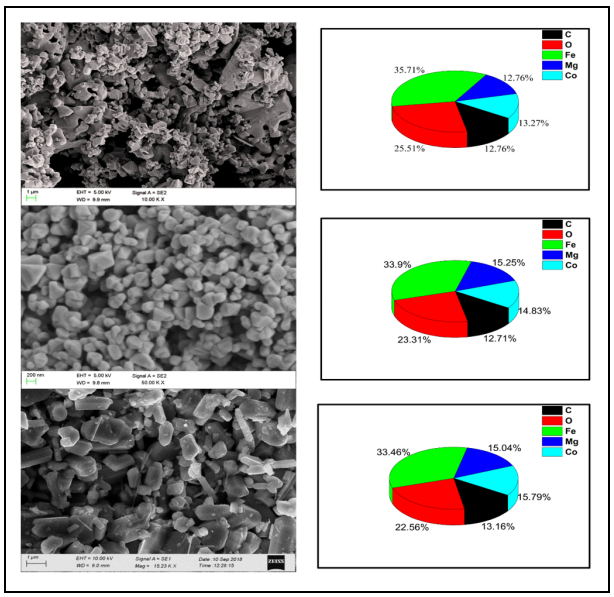


Fig. 2: FESEM-EDS of $Fe_{1-2x}Mg_xCo_x$ nanoparticles for S_1, S_2 and S_3

3.2 FESEM-EDS Analysis

The FESEM images were recorded at different magnifications to study the morphology and size of the $Fe_{1-2x}Mg_xCo_x$ nanoparticles (Fig. 3.2). From the images, it is evident that the formation of the nanoparticles is in tetragonal-like morphology due to aggregation, while XRD confirms a cubic maghemite crystal structure. The difference arises because FESEM reflects surface morphology, whereas XRD indicates decreasing crystallographic arrangement and agglomeration of particles with the increase of concentration from sample S1 to S3. The particle size was found to be 44 nm (S1), 48 nm (S2), 51 nm(S3), and further, the FESEM confirms the formation of high-density bio-reduced $Fe_{1-2x}Mg_xCo_x$ nanoparticles from the *Psidium guajava* plant extract.

The elemental composition of the as-synthesized $Fe_{1-2x}Mg_xCo_x$ nanoparticles was determined by EDS spectrum, and the bar diagram for each sample is shown in Fig. 2. From the bar diagram, it is evident that the presence of Fe, Mg, and Co was confirmed with an average of 33-35% of iron and 12-15% of the remaining dopants for each sample. The presence of C in the nanoparticles may be due to the bio-components present in the *Psidium guajava* plant extract used to reduce the metal ions, and the presence of O was due to the oxidation during the formation of FeO. Hence, EDS analysis confirms that the biomolecules in the plant extract were responsible for the formation of nanoparticles.

3.3 UV-visible Analysis

Fig. 3 shows the UV visible spectra of $Fe_{1-2x}Mg_xCo_x$ nanoparticles. From the spectra, the absorption bands at 362 nm (S1), 367 nm (S2), and 368 nm (S3) were observed, indicating the formation of nanoparticles with the presence of maghemite. As the intensity of the absorption band increases very slightly with the concentration, a small red shift is observed in the spectrum.

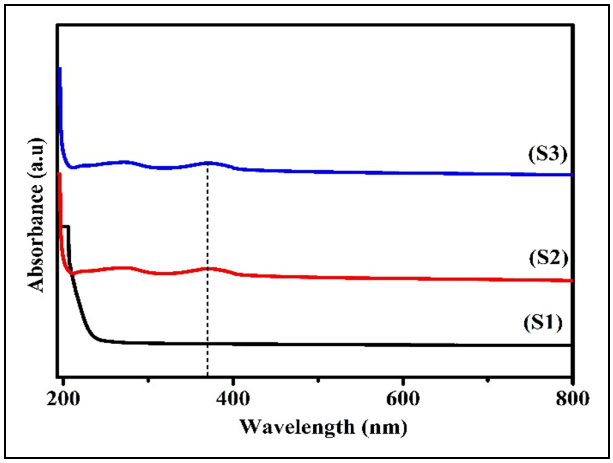


Fig. 3: FESEM-EDS of $Fe_{1-2x}Mg_xCo_x$ nanoparticles for S_1, S_2, S_3

3.4 FT-Raman and FTIR Analysis

Raman spectroscopy was employed to study the nature, rotational, and vibrational modes of the synthesized $Fe_{1-2x}Mg_xCo_x$ nanoparticles for all three samples. Fig. 4(a) shows the Raman spectrum of each sample for the nanoparticles recorded at room temperature with an excitation laser wavelength of 785 nm. The peaks were observed at 730 nm, identified for the FeO phonon mode, 518 nm for MgO, and 321 nm for Co_3O_4 vibrational modes. As the intensity of the parent material FeO is higher than the other two dopants for all the concentrations hence its presence is evident. The functional groups, biological entities, and the chemical bonds of the synthesised $Fe_{1-2x}Mg_xCo_x$ nanoparticles were analysed through FTIR spectroscopy, which was recorded in the range 4000-500cm^{-1} as shown in Fig. 4(b). From the spectrum, the infrared absorption peaks were identified at 3440 cm^{-1} belongs to O-H stretching bonds, 1645 cm^{-1}, and 1396 cm^{-1}, corresponds to amide and hydroxyl group in the ring, respectively. At 920 cm^{-1} C-O bond was observed, and at 528 cm^{-1}, the peak represents the presence of the FeO vibrational bond of maghemite structure, indicating the formation of nanoparticles. As the concentration increases from

sample S1 to S3, the peak of FeO gets broader; hence, the broad peak for S3 indicates strong interactions of hydrogen bonding, which can result in a small particle size with less agglomeration. Hence, from the spectrum, it is clear that the metal ions have been reduced due to the bio-components present in the plant extract and stabilize the $Fe_{1-2x}Mg_xCo_x$ nanoparticles.

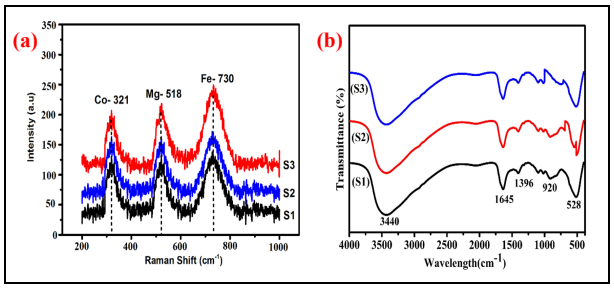


Fig. 4: (a) FT-Raman spectrum and (b) FTIR spectrum of $Fe_{1-2x}Mg_xCo_x$ nanoparticles S_1, S_2, S_3

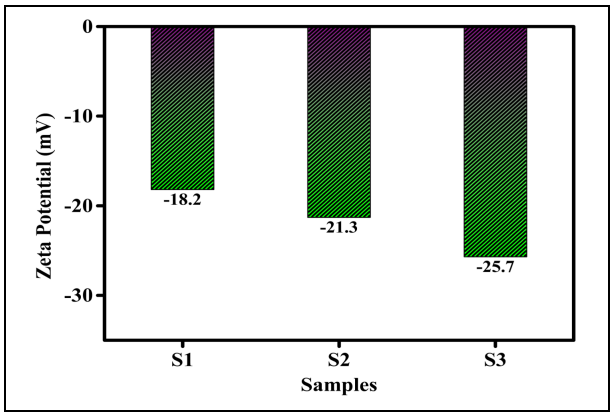


Fig. 5: Variation in the zeta potential of $Fe_{1-2x}Mg_xCo_x$ nanoparticles

3.5 Zeta Potential

The bio-reduced $Fe_{1-2x}Mg_xCo_x$ nanoparticles were subjected to study their stability and presence of surface charge by zeta potential analysis. Fig. 5 shows the bar graph depicting the variation of zeta potential with respect to the synthesized nanoparticles for samples S1, S2, and S3, which reveals that the particles carry negative charge of -18.2 mV (S1), -21.3 mV (S2), and -25.7 mV (S3), indicating the stability of the nanoparticles was very strong at room temperature. And also, the reason for the small particle size may be due to the repulsive forces arising from the negative charge of the particles. As the small particle size with a large negative zeta potential was found to be more propitious, as it can easily target the affected molecules in drug delivery.

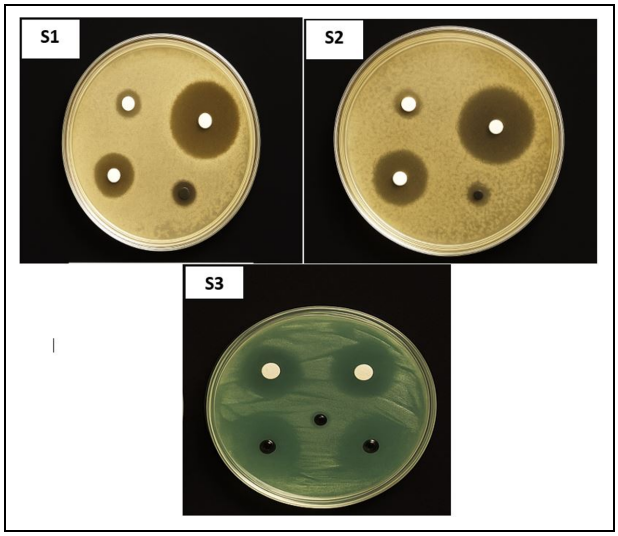


Fig. 6: Agar diffusion plates of antibacterial activity of (a) Listeria monocytogenes and (b) Serratia marcescens for $Fe_{1-2x}Mg_xCo_x$ nanoparticles (S_1, S_2, S_3)

3.6 Antibacterial Studies

Agar-well diffusion assay was carried out to study the bactericidal property of $Fe_{1-2x}Mg_xCo_x$ nanoparticles against *Listeria monocytogenes* (Gram positive) and *Serratia marcescens* (Gram negative) and zone of inhibition was measured for three concentrations (60 µg/mL, 40 µg/mL, and 20 µg/mL) of each sample of nanoparticles S1, S2 and S3. An increase in inhibition zone was observed for both organisms as the concentration of nanoparticles increased, but for *Listeria monocytogenes*, the bactericidal activity is more than that of *Serratia marcescens* (Table 3). The stronger effect against Gram-positive bacteria such as *L. monocytogenes* may be due to their thinner peptidoglycan layer, allowing easier nanoparticle penetration, while Gram-negative bacteria possess an outer membrane that restricts diffusion (Hassan *et al.* 2022), although for sample S3 with a concentration of 60 µg/mL, the effectiveness was very high. Hence, $Fe_{1-2x}Mg_xCo_x$ nanoparticles showed significant bactericidal activity. Fig. 6(i) shows the agar-diffusion method carried out for two bacterial agents, in which it can be noted that for both *Listeria monocytogenes* (Gram positive) and *Serratia marcescens* (Gram negative), the nanoparticles showed a considerable antibacterial activity but for sample S3 (x=0.1) showed higher dead bacteria (%) with more concentration of nanoparticles (60 µg/mL). Fig. 7 (a) and (b) show the graphical representation of antibacterial activity, which provides a pictorial representation for different concentrations of samples.

Table 1. Zone of inhibition for antibacterial test of $Fe_{1-2x}Mg_xCo_x$ nanoparticles

Organisms	Zone of Inhibition(mm) Mean ± SD									Control Drug
	Sample S_1			Sample S_2			Sample S_3			
	20 µg/mL	40 µg/mL	60 µg/mL	20 µg/mL	40 µg/mL	60 µg/mL	20 µg/mL	40 µg/mL	60 µg/mL	
Listeria monocytogene	11± 1.6	15±3.2	18± 1.4	9± 1.9	15± 2.5	19± 2.6	14± 1.5	18±2.3	21±2.8	13± 1.9
Serratia marcescens	12± 1.3	13± 1.8	16± 2.4	7± 2.7	12± 2.3	15± 2.5	12± 2.8	15± 3.1	17± 3.3	15± 1.5

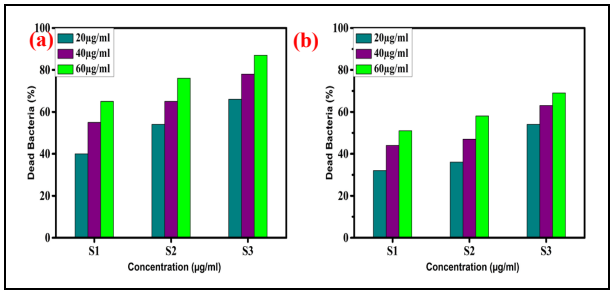


Fig. 7: Antibacterial activity of (a) *Listeria monocytogenes* and (b) *Serratia marcescens* for $Fe_{1-2x}Mg_xCo_x$ nanoparticles (S_1, S_2, S_3)

3.7 *In vitro* Cytotoxicity

Investigation of *in vitro* cytotoxicity through MTT assay for the as-synthesized $Fe_{1-2x}Mg_xCo_x$ nanoparticles was carried out against two cancer cell lines, namely MCF-7 and HeLa cells, at different concentrations of each sample, S1, S2, and S3. The IC_{50} values and the cell viability were measured, which were found to decrease with an increase in concentration of nanoparticles in a dose-dependent manner for all three samples, as can be seen in Table 1. The IC_{50} values found to be 51.54 µg/mL (S1), 44.70 µg/mL (S2), 40.13 µg/mL (S3) for HeLa cell lines and 63.73 µg/mL, 56.67 µg/mL (S2), 50.52 µg/mL (S3) for MCF-7 cell lines, showing that the $Fe_{1-2x}Mg_xCo_x$ nanoparticles can act as a promising anticancer agent for both cell lines, but for HeLa cells the effectivity was more compared to MCF-7 cells. Sample S3 exhibits minimum values of 40.13 µg/mL (HeLa) and 50.52 µg/mL (MCF-7). Further, to compare this cytotoxicity with the normal cells, MTT assay was carried out against Vero cells for the nanoparticles in a similar way, because for nanoparticles to act as an efficient drug, they should harm only damaged cells without affecting the normal cells. The IC_{50} values for the Vero cells were found to be 90.27 µg/mL (S1), 105.8 µg/mL (S2), 110.4 µg/mL (S3), which confirm the non-toxic nature of the synthesized nanoparticles against normal lines. A graph was plotted for all the cell lines for concentration versus cell viability (%) as shown in Fig. 8 (a)(b)(c) and for more clarity, 3D bar graph shown in Fig. 8(d) which was plotted to understand the anticancer activity of the nanoparticles. The combined antibacterial and anticancer properties indicate their multifunctional behavior and potential application in biomedicine. The results are consistent with other reports on green-synthesized Fe-based nanoparticles displaying similar dual activities (Zhang *et al.* 2020).

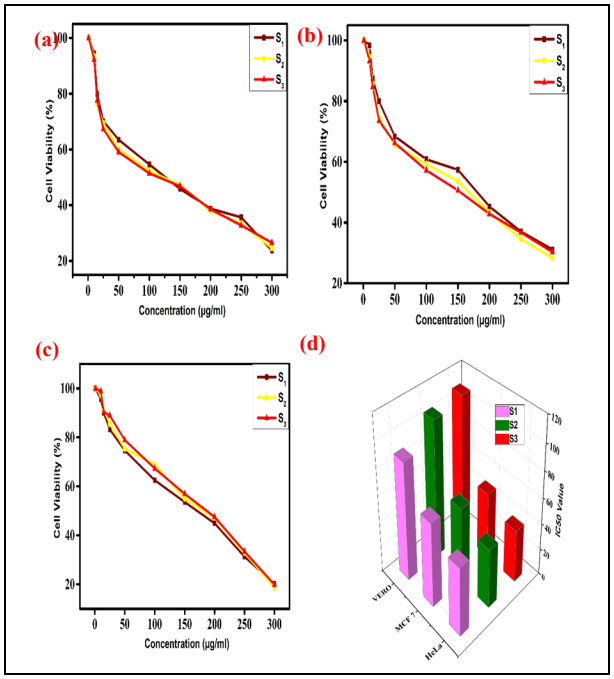


Fig. 8: *In vitro* anticancer activity of (a)HeLa cells (b)MCF-7 cells (c)Vero cells and (d) Plot against IC_{50} values versus cancer cells for $Fe_{1-2x}Mg_xCo_x$ nanoparticles (S_1, S_2, S_3)

Table 2. MTT assay test of synthesized $Fe_{1-2x}Mg_xCo_x$ nanoparticles (S_1, S_2, S_3)

Concentration (µg/mL)	Cell Viability (%)								
	HeLa Cells			MCF-7 Cells			Vero Cells		
	S_1	S_2	S_3	S_1	S_2	S_3	S_1	S_2	S_3
300	23.67	24.56	26.54	31.12	28.39	30.26	20.14	18.71	20.91
250	35.62	33.49	32.78	36.98	34.57	36.72	31.27	32.87	36.82
200	38.75	37.92	38.49	45.31	43.34	42.83	44.92	47.23	44.72
150	45.82	47.24	46.82	57.34	53.67	50.57	53.59	55.03	58.31
100	54.63	52.38	51.42	60.84	59.26	57.23	62.5	68.92	64.87
50	63.48	60	59.06	68.35	65.48	66.22	74.65	75.38	71.98
25	70.2	69.43	67.29	79.94	74.28	73.48	83.22	85.5	78.34
15	79.99	76.29	77.53	87.48	85.72	84.59	89.9	91.26	88.32
10	94.56	93.46	92.3	98.33	94.56	93.21	95.49	97.34	96.23
Control	100	100	100	100	100	100	100	100	100
IC_{50} Value (µg/mL)	51.54	44,70	40.13	63.73	56.67	50.52	90.27	105.8	110.4

4. CONCLUSION

$Fe_{1-2x}Mg_xCo_x$ nanoparticles were prepared using *Psidium guajava* plant extract, and their antibacterial and anticancer properties were studied. The plant extract was used as a stabilizing and reducing agent in the formation of nanoparticles. $Fe_{1-2x}Mg_xCo_x$ nanoparticles showed bactericidal activity against *Listeria monocytogenes* and *Serratia marcescens* strains. The *in vitro* cytotoxic effect against cancer cells of the nanoparticles gave proof for their high potency to act as a powerful drug. The efficacy of cancer cells of MCF-7 and HeLa cells was comparably efficient, and the nanoparticles showed good efficacy against HeLa cells. Also, the $Fe_{1-2x}Mg_xCo_x$ nanoparticles were not toxic to normal cells, as they showed no efficacy against Vero normal cell lines.

FUNDING

This research received no specific grant from any funding agency in the public, commercial, or not-for-profit sectors.

CONFLICTS OF INTEREST

The authors declare that there is no conflict of interest.

COPYRIGHT

This article is an open-access article distributed under the terms and conditions of the Creative Commons Attribution (CC BY) license (http://creativecommons.org/licenses/by/4.0/)

REFERENCES

Anastas, P. T. and Warner, J. C., Green Chemistry: Theory and Practice, Oxford University Press, New York, 1998.

Anderson, S. D., Gwenin, V. V. and Gwenin, C. D., Magnetic Functionalized Nanoparticles for Biomedical, Drug Delivery and Imaging Applications, *Nanoscale Res. Lett.,* 14(1), 188(2019). https://doi.org/10.1186/s11671-019-3019-6

Arima, H. and Danno, G. I., Isolation of antimicrobial compounds from guava (*Psidium guajava* l.) and their structural elucidation, *Biosci. Biotechnol. Biochem.,* 66(8), 1727–1730(2002) https://doi.org/10.1271/bbb.66.1727

Armendariz, V., Herrera, I., Videa, J. R. P., Yacaman, M. J., Troiani, H., Santiago, P. and Torresdey, J. L. G., Size controlled gold nanoparticle formation by Avena sativa biomass: Use of plants in nanobiotechnology, *J. Nanopart. Res.,* 6(4), 377–382(2004). https://doi.org/10.1007/s11051-004-0741-4

Banerjee, P., Satapathy, M., Mukhopahayay, A. and Das, P., Leaf extract mediated green synthesis of silver nanoparticles from widely available Indian plants: Synthesis, characterization, antimicrobial property and toxicity analysis, *Bioresour. Bioprocess.,* 1(1), 3(2014). https://doi.org/10.1186/s40643-014-0003-y

Chambers, E. and Mitragotri, S., Long circulating nanoparticles via adhesion on red blood cells: Mechanism and extended circulation, *Exp. Biol. Med.,* 232(7), 958–66(2007).

Chou, S. W., Shau, Y. H., Wu, P. C., Yang, Y. S., Shieh, D. B. and Chen, C. C., In Vitro and in Vivo Studies of FePt Nanoparticles for Dual Modal CT-MRI Moelcular Imaging, *J. Am. Chem, Soc.,* 132(38), 13270–13278(2010). https://doi.org/10.1021/ja1035013

Devi, H. S. and Singh, T. D., Synthesis of Copper Oxide Nanoparticles by a Novel Method and its Application in the Degradation of Methyl Orange, *Adv. Electron. Electr. Eng.,* 4(1), 83–88 (2014).

Feynman, R. P., There's Plenty of Room at the Bottom, Eng. Sci., 23(5), 22–36 (1960)

Gao, X., Cui, Y., Levenson, R. M., Chung, L. W. K. and Nie, S., In vivo cancer targeting and imaging with semiconductor quantum dots, *Nat. Biotechnol.,* 22(8), 969–976(2004). https://doi.org/10.1038/nbt994

Gutiérrez, R. M. P., Mitchell, S. and Solis, R. V., *Psidium guajava*: A review of its traditional uses, phytochemistry and pharmacology, *J. Ethnopharmacol.,* 117(1), 1–27(2008). https://doi.org/10.1016/j.jep.2008.01.025

Hamidi, M., Azadi, A. and Rafiei, P., Hydrogel nanoparticles in drug delivery, *Adv. Drug Deliv. Rev.,* 60(15), 1638–1649(2008). https://doi.org/10.1016/j.addr.2008.08.002

Haverkamp, R. G. and Marshall, A. T., The mechanism of metal nanoparticle formation in plants: Limits on accumulation, *J. Nanopart Res.,* 11(6), 1453–1463(2009). https://doi.org/10.1007/s11051-008-9533-6

Huh, Y. M., Jun, Y. W., Song, H. T., Kim, S., Choi, J. S., Lee, J. H., Yoon, S., Kim, K. S., Shin, J. S., Suh, J. S. and Cheon, J., In vivo magnetic resonance detection of cancer by using multifunctional magnetic nanocrystals, *J. Am. Chem. Soc.,* 127(35), 12387–12391(2005). https://doi.org/10.1021/ja052337c

Iconaru, S. L., Prodan, A. M., Coustumer, P. L. and Predoi, D., Synthesis and antibacterial and antibiofilm activity of iron oxide glycerol nanoparticles obtained by coprecipitation method, *J. Chem.,* 2013(1), 412079(2013) https://doi.org/10.1155/2013/412079

Kalu, O., Correia, M. R., Cantarero, A., Rodriguez, H. A. M., Moller, J. A. D. and Rojas, A. R., Enhanced optical properties of Cd–Mg-co-doped ZnO nanoparticles induced by low crystal structure distortion, *J. Phys. Chem. Solids.,* 146, 109611(2020). https://doi.org/10.1016/j.jpcs.2020.109611

Khalkhali, M., Mohammadinejad, S., Khoeini, F. and Rostamizadeh, K., Vesicle-like structure of lipid-based nanoparticles as drug delivery system revealed by molecular dynamics simulations, *Int. J. Pharm.,* 559, 173–181(2019). https://doi.org/10.1016/j.ijpharm.2019.01.036

Labhasetwar, V. and Leslie-Pelecky, D. L., Biomedical Applications of Nanotechnology, Wiley-Interscience, Hoboken, NJ, 2007

Maliekkal, B. P., Kakkassery, J. T. and Palayoor, V. R., Efficacies of sodium nitrite and sodium citrate–zinc acetate mixture to inhibit steel rebar corrosion in simulated concrete interstitial solution contaminated with NaCl, *Int. J. Ind. Chem.,* 9(2), 105–114(2018). https://doi.org/10.1007/s40090-018-0142-7

Narayanan, K. B. and Sakthivel, N., Coriander leaf mediated biosynthesis of gold nanoparticles, *Mater. Lett.,* 62(30), 4588–4590(2008). https://doi.org/10.1016/j.matlet.2008.08.044

Navaladian, S., Viswanathan, B., Viswanath, R. P. and Varadarajan, T. K., Thermal decomposition as route for silver nanoparticles, *Nanoscale Res. Lett.,* 2(1), 44(2007). https://doi.org/10.1007/s11671-006-9028-2

Paull. R., Wolfe, J., Hébert, P. and Sinkula, M., Investing in nanotechnology, *Nat. Biotechnol.,* 21(10), 1144–7(2003). https://doi.org/10.1038/nbt1003-1144

Phanjom, P. and Ahmed, G., Biosynthesis of Silver Nanoparticles by Aspergillus oryzae (MTCC No. 1846) and Its Characterizations, *Nanosci. Nanotechnol.,* 5(1), 14–21(2015). https://doi.org 10.5923/j.nn.20150501.03

Philip, D. and Unni, C., Extracellular biosynthesis of gold and silver nanoparticles using Krishna tulsi (Ocimum sanctum) leaf, *Physica E.,* 43(7), 1318–1322(2011). https://doi.org/10.1016/j.physe.2010.10.006

Phokha, S. and Seraphin, S., Indium oxide (In_2O_3) nanoparticles using Aloe vera plant extract: Synthesis and optical properties, *Mater. Sci. Semicond. Process.,* 31, 161–165 (2015).

Popovic, N. and Brundin, P., Therapeutic potential of controlled drug delivery systems in neurodegenerative diseases, *Int. J. Pharm.,* 314(2), 120–126(2006). https://doi.org/10.1016/j.ijpharm.2005.09.040

Prathna, T. C., Chandrasekaran, N., Raichur, A. M. and Mukherjee, A., Biomimetic synthesis of silver nanoparticles by Citrus limon (lemon) aqueous extract and theoretical prediction of particle size, *Colloids Surf. B.,* 82(1), 152–159(2011). https://doi.org/10.1016/j.colsurfb.2010.08.036

Pu, X., Zhao L, Li J, Song R, Wang Y, Yu K, Hou X, Qiao P, Zong L and Chang S 2019 A polymeric micelle with an endosomal pH-sensitivity for intracellular delivery and enhanced antitumor efficacy of hydroxycamptothecin, *Acta Biomater.,* 88, 357–369(2019). https://doi.org/10.1016/j.actbio.2019.02.039

Raj, S., Mali, S. C. and Trivedi, R., Green synthesis and characterization of silver nanoparticles using Enicostemma axillare (Lam.) leaf extract, *Biochem. Biophys. Res. Commun.,* 503(4), 2814–2819(2018). https://doi.org/10.1016/j.bbrc.2018.08.045

Rajendran, R., et al. Plant-mediated synthesis of Fe-based nanoparticles: Advances and biomedical applications, *J. Environ. Nanotechnol*., 13(2), 45–60(2024). https://doi.org/10.1016/j.jenvnano.2024.02.005

Ramos, A. P., Cruz, M. A. E., Tovani, C. B. and Ciancaglini, P., Biomedical applications of nanotechnology, *Biophys. Rev.,* 9(2), 79–89(2017). https://doi.org/10.1007/s12551-016-0246-2

Ramteke, C., Chakrabarti, T., Sarangi, B. K. and Pandey, R., Synthesis of Silver Nanoparticles from Plant Extract and Its Application in Cancer Treatment, *Int. J. Green Nanotechnol.*, 1(1), 108–114 (2013).

Saji, V. S., Choe, H. C. and Yeung, K. W. K., Nanotechnology in biomedical applications: A review, *Int. J. Nano Biomater*., 3(2), 119(2010). https://doi.org/10.1504/IJNBM.2010.037801

Salata, O. V., Applications of Nanoparticles in Biology and Medicine, *J. Nanobiotechnol*., 2(1), 3 (2004).

Sengupta, S., Eavarone, D., Capila, I., Zhao, G., Watson, N., Kiziltepe, T. and Sasisekharan, R., Temporal targeting of tumour cells and neovasculature with a nanoscale delivery system, *Nat.,* 436(7050), 568–572(2005). https://doi.org/10.1038/nature03794

Shankar, S. S., Rai, A., Ahmad, A. and Sastry, M., Controlling the optical properties of lemongrass extract synthesized gold nanotriangles and potential application in infrared-absorbing optical coatings, *Chem. Mater.,* 17(3), 566–572(2005). https://doi.org/10.1021/cm048292g

Shevchenko, E. V., Talapin, D. V., Schnablegger, H., Kornowski, A., Festin, Ö., Svedlindh, P., Haase, M. and Weller, H., Study of nucleation and growth in the organometallic synthesis of magnetic alloy nanocrystals: The role of nucleation rate in size control of $CoPt_3$ nanocrystals, *J. Am. Chem. Soc.,* 125(30), 9090–9101(2003). https://doi.org/10.1021/ja029937l

Singh, J., Dutta, T., Kim, K. H., Rawat, M., Samddar, P. and Kumar, P., "Green" synthesis of metals and their oxide nanoparticles: Applications for environmental remediation, *J. Nanobiotechnol.,* 16(1), 84(2018). https://doi.org/10.1186/s12951-018-0408-4

Srinoi, P., Chen, Y. T., Vittur, V., Marquez, M. D. and Lee, T. R., Bimetallic nanoparticles: Enhanced magnetic and optical properties for emerging biological applications, *Appl. Sci.,* 8(7), 1106(2018). https://doi.org/10.3390/app8071106

Saeed, T., Tabatabaei, S. M., Ghaffari, Y. and Esmaeili, A., Living Plant-Mediated Synthesis of Nanoparticles, *J. Adv. Med. Sci. Appl. Technol*., 4(1), 2–7 (2018). https://doi.org/10.32598/jamsat.4.1.1

Sutapa, I. W., Wahab, A. W., Taba, P. and Nafie, N., Synthesis and structural profile analysis of the MgO nanoparticles produced through the sol-gel method followed by annealing process, *Orient. J. Chem.,* 34 1016–25(2018). https://doi.org/10.13005/ojc/340252

Tan, J. P. K., Voo, Z. X., Lim, S., Venkataraman, S., Ng, K. M., Gao, S., Hedrick, J. L. and Yang, Y. Y., Effective encapsulation of apomorphine into biodegradable polymeric nanoparticles through a reversible chemical bond for delivery across the blood–brain barrier, *Nanomed. Nanotechnol. Biol. Med.,* 17, 236–245(2019) https://doi.org/10.1016/j.nano.2019.01.014

Torresdey, J. L. G., Parsons, J. G., Gomez, E., Videa, J. P., Troiani, H. E., Santiago, P. and Yacaman, M. J., Formation and Growth of Au Nanoparticles inside Live Alfalfa Plants, *Nano Lett.,* 2(4), 397–401(2002). https://doi.org/10.1021/nl015673+

Venugopal, G., Green synthesis of silver nanoparticles from *Psidium guajava* leaves and its antibacterial activity, *Int. J. Bioassays.,* 6(7), 5441(2017). https://doi.org/10.21746/ijbio.2017.07.003

Vinod, V. T. P., Saravanan, P., Sreedhar, B., Devi, D. K. and Sashidhar, R. B., A facile synthesis and characterization of Ag, Au and Pt nanoparticles using a natural hydrocolloid gum kondagogu (Cochlospermum gossypium), *Colloids Surf., B.,* 83(2), 291–298(2011). https://doi.org/10.1016/j.colsurfb.2010.11.035

Xu, C., Liang, Z., Tang, D., Xiao, T., Tsunoda, M., Zhang, Y., Zhao, L., Deng, S. and Song, Y., Gas chromatography-mass spectrometry (GCMS) analysis of volatile components from guava leaves, *J. Essent. Oil Bear. Plants.,* 20(6), 1536–1546(2017). https://doi.org/10.1080/0972060X.2017.1417746

Yamamoto, Y., Tamura, S., Kumon, T., Mizuno, K., Nakagawa, K., Hashimoto, M. and Kanazawa, S., Synthesis of Indium Oxide Nanoparticles Using Aloe vera Plant Extract and Their Optical Properties, *J. Mater. Sci. Mater. Electron.,* 18(2), 126–131 (2007).

Yin, S., Li, Z., Cheng, L., Wang, C., Liu, Y., Chen, Q., Gong, H., Guo, L., Li, Y. and Liu, Z., Magnetic PEGylated Pt_3Co nanoparticles as a novel MR contrast agent: In vivo MR imaging and long-term toxicity study, *Nanoscale.,* 5(24), 12464(2013). https://doi.org/10.1039/C3NR04212J

Zahin, N., Anwar, R., Tewari, D., Kabir, T., Sajid, A. Mathe ofolew, B., Uddin, M. S., Aleya, L. and Daim, M. M. A., Nanoparticles and its biomedical applications in health and diseases : special focus on drug delivery, *Environ. Sci. Pollut. Res.,* 27(16), 19151-19168(2020). https://doi.org/10.1007/s11356-019-05211-0